sciendo
ISSN 1335-8871
MEASUREMENT SCIENCE REVIEW
Journal homepage: https://content.sciendo.com

# A Novel Non-Contact Measurement Method of Ball Screw Thread Profile Detection Based on Machine Vision

Bing-yi Miao[1*], Xian-cheng Wang[1], Jun-hua Chen[1], Chu-hua Jiang[1], Meng-yao Qu[2]

[1]*College of Science & Technology Ningbo University, Wenwei Road, No.521, 315211, Cixi, China, miaobingyi@nbu.edu.cn*
[2]*Ningbo Institute of Technology of Zhejiang University, Qianhunan Road, No.1, 315100, Ningbo, China*

Abstract: The transmission accuracy of the ball screw depends on the processing quality of the thread profile. Traditional detection method of thread profile is complicated and inefficient. When shooting the thread profile of the ball screw in the normal section, the camera axis must be tilted to the lead angle, and adjustment errors are easily introduced from both the front view and the top view. When shooting in the axial section, the spiral lines block each other, so the actual thread profile cannot be captured for detection. In order to solve the above problems, a thread profile detection method is proposed: the theoretical equation of the ball screw thread profile in the axial section is derived based on the theoretical thread profile in the normal section, and the theoretical equation of the thread profile projection curve in the axial section is solved based on helix analysis, and the differential equation between them is obtained; then, the theoretical correction value of the thread profile projection curve is obtained by Linear Search to find the boundary value; the actual thread profile in both axial section and normal section is finally obtained with the theoretical correction value, which can support accurate measurement and detection of the key parameters of the thread profile. Experiments show that the proposed method can effectively improve the accuracy of the ball screw thread profile detection.

Keywords: Ball screw thread detection, thread profile on axis section, thread profile projection curve on axial section, thread profile on normal section, machine vision.

## 1. INTRODUCTION

The ball screw pair is a highly efficient and reliable mechanical transmission component, which can transform rotary motion into linear motion and is widely used in the field of CNC machine tools, as in [1], [2]. The transmission accuracy of the ball screw depends on the processing quality of the thread. Therefore, it is necessary to detect the thread of the ball screw accurately and efficiently.

The traditional detection method is manual contact measurement using equipment, but it has the following two disadvantages: (1) the detection process is complicated and it makes high demands on the workers' professional level, which reduces efficiency; (2) contact measurement causes some damage to the surface of the thread and affects its quality. With the development of computer technology, non-contact detection through machine vision solutions is currently the main research trend, the main process is collecting the optical image of the object to be detected, then using image processing technology to extract and quantify the feature, obtaining the result of detection.

At present, many relevant scholars at home and abroad have conducted research on this subject and have already formed a relatively complete thread detection system, as in [3]-[8], which can be described as follows: First, the original image of the thread profile by CCD or other optical camera is captured, then the features of thread profile based on image processing techniques such as filtering, boundary extraction and curve fitting are extracted, and finally the parameters are measured from the acquired features such as the thread profile, which are considered as the result of detection. Min and Zhao respectively designed a non-contact thread parameter measurement system based on machine vision to support efficient and accurate measurement of the thread contact angle, as in [9], [10]; Rao et al. summarized the image processing technology and computer vision algorithms currently used for external thread detection, as in [11]; Senthilnathan used a diffuse reflection light source to obtain a thread profile projection, and proposed a profile processing algorithm to estimate the thread parameters, as in [12]; Chen et al. integrated the photoelastic effect and an image processing algorithm to measure the contact angle of the ball screw, as in [13]; Li et al. proposed a Res Unet-based thread edge recognition method that eliminates the need for thread area calibration and identifies the thread edge in a complex environment, as in [14]; Chen took the possible thread shape distortion during CCD shooting into account, and gave a corresponding compensation algorithm for the image distortion on the optical angle, as in [15].

However, the above solutions are only applied to the detection of ordinary threads with a linear profile, while the

DOI: 10.2478/msr-2023-0006
*Corresponding author: miaobingyi@nbu.edu.cn (B. Miao)

thread profile of the ball screw is a curve, which is more difficult to detect. As far as we know, there are few studies on the thread profile of ball screws.

## 2. DIFFICULTY ANALYSIS OF BALL SCREW THREAD DETECTION

For ball screw detection, the conventional method is to measure parameters such as outer diameter and pitch, but the thread profile is more important. According to the definition in [16], the allowable error of thread raceway profile refers to the maximum deviation between the actual thread profile and the standard thread profile. For a single arc raceway ball screw, mainly the radius deviation of the raceway is detected.

The ratio between the raceway radius $r_b$ on the normal section and the ball radius $r$ affects the bearing capacity of the ball screw transmission, as shown in Fig. 1. If the ratio is too large, it will cause heavy friction loss; if the ratio is too small, the load-bearing capacity will be reduced. The single arc raceway ball screw usually takes $r_b = 1.04r$ . In the acceptance test of the P5 grade ball screw most commonly used in China, the allowable error of the thread profile is ±0.02 mm.

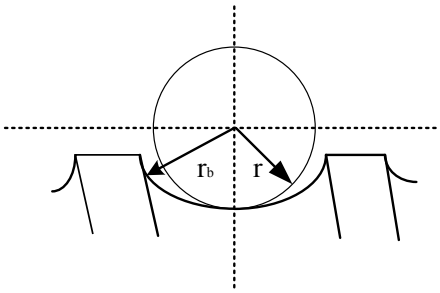


Fig. 1. Correspondence of thread profile and ball.

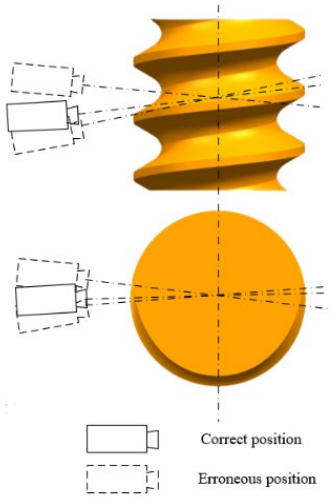


Fig. 2. Rotating axis shooting state of the camera.

In order to obtain the thread profile in the normal section, it is usually necessary to rotate the camera axis by a lead angle for shooting, as in [17], as shown by the camera position drawn by a solid line in Fig. 2. In the detection process, it is difficult to ensure the accuracy of the camera axis in space. As shown by the camera position drawn by a dotted line in Fig. 2, from the main view, the camera axis is easy to shift up and down. Similarly, from the top view, the camera axis can easily shift left and right. Once there is an error in the angle adjustment, the accurate thread profile cannot be obtained in the normal section.

In order to avoid detection errors caused by the rotation of the camera axis, when the ball screw is fixed, it is easy to obtain the thread profile in the axial section as long as the camera axis is orthogonal to the ball screw axis, as shown in Fig. 3. By reversely deriving the radius of curvature of the thread profile in the normal section from the thread profile in the axial section, it is possible to determine whether the profile is qualified.

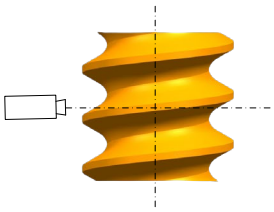

Fig. 3. Orthogonal shooting state of the camera.

Since multiple spiral lines on the raceway surface block each other during the spiraling process, as shown in Fig. 4, the curve of the thread profile in the axial section captured by the camera is not a true thread profile, but a thread profile projection curve that requires further correction. The comparison between them is shown in Fig. 5, Curve-1 is the thread profile projection curve while Curve-2 is the actual thread profile. Some researchers have proposed correction algorithms for the thread profile projection curve of ordinary threads with straight thread profile, as in [18], [23]. Meanwhile, for ball screw, the thread profile in the axial section is a curve, which makes the correction more difficult, and only a few researchers have studied it.

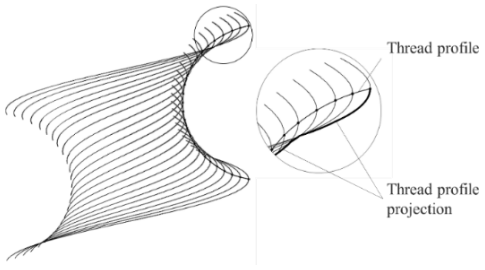


Fig. 4. Contrast between thread profile in the axial section and spiral projection boundary.

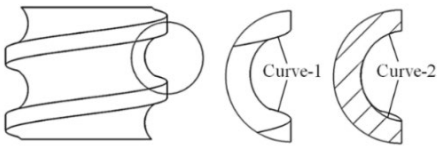


Fig. 5. Thread profile and thread profile projection curve in the axial section.

To deal with the difficulties above, the research method proposed is shown in Fig. 6.

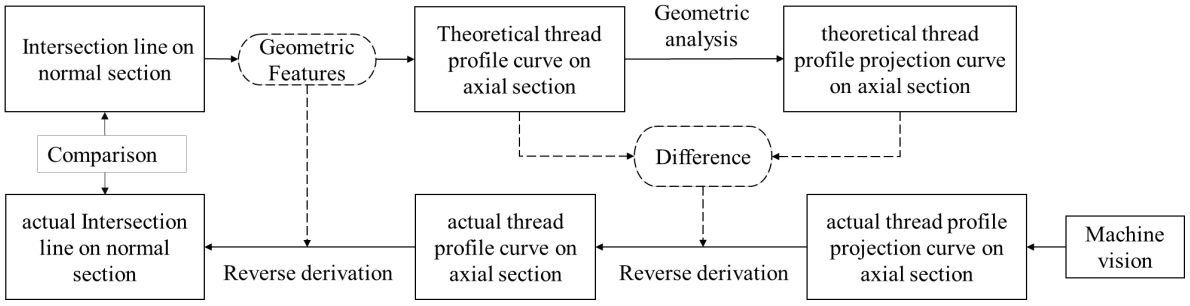


Fig. 6. Ball screw thread profile detection method based on the thread profile curve in the axial section.

First: Based on the geometric features of the theoretical thread profile in the normal section, the theoretical thread profile in the axial section is derived. Second: Through geometric analysis of the occlusion phenomenon of the theoretical thread profile in the axial section, the theoretical thread profile projection curve is established, and the difference equation between the theoretical thread profile and the thread profile projection curve in the axial section is obtained. This part of the content is expanded in Section 3 and Section 4.

Then, the thread profile projection curve in the axial section is captured with a CCD camera and corrected using the differential equation mentioned above. Thus, the actual thread profile in the axial section is obtained, which can be used to reversely derive the radius of curvature of the actual thread profile in the normal section. By comparing the actual radius with the standard value, it is determined whether the thread profile of the ball screw is qualified. This part of the content is expanded in Section 5.

## 3. THEORETICAL THREAD PROFILE IN AXIAL SECTION

In order to measure the parameters of the ball screw, it is first necessary to establish a standard curve equation of the thread profile in the axial section based on the theoretical thread profile in the normal section, which provides a theoretical model basis for the subsequent correction process.

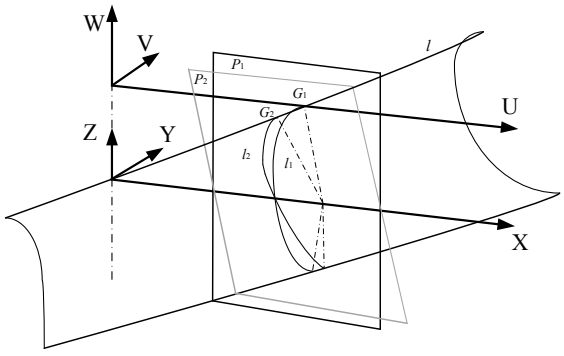


Fig. 7. Relationship between the thread profile raceway, the normal section, and the axial section.

As shown in Fig. 7, take the axial section $P_1$ and the normal section $P_2$ at any point on the raceway. The intersection of $P_1$ and the raceway is $l_1$, the intersection of $P_2$ and the raceway is $l_2$, and $l_2$ is a standard arc. Take a helix $l$ of the raceway as research object, $l$ and $l_1$, $l_2$ intersect at points $G_1$ and $G_2$, respectively. Take the intersection of $P_1$ and $P_2$ as X-axis and the axis of the spiral as the Z-axis. The coordinate system XYZ is established. Taking the axis parallel to the X-axis and passing through $G_1$ as U-axis, and the spiral axis as the W-axis, a coordinate system UVW is established to study the curves $l_1$ and $l_2$, as shown in Fig. 7 and Fig. 8.

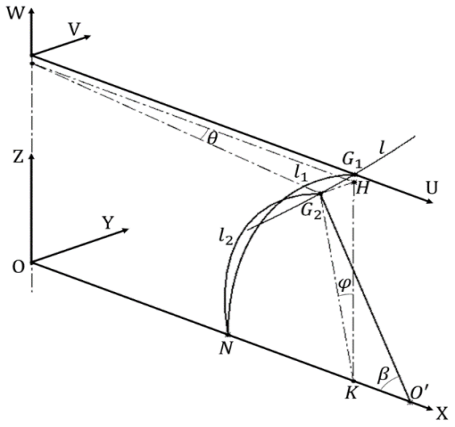


Fig. 8. Relationship between $l_1$-thread profile in the axial section and $l_2$- thread profile in the normal section.

Give the outer diameter-$d_1$, the minor diameter-$d_2$, the lead angle-$\varphi$, the pitch $p$ and the curvature radius of the normal section arc of the ball screw-$r_\mathrm{b}$. Assume $O'$ is the center of $l_2$, N is the intersection point of $l_1$, $l_2$ and A-axis, $H$ and $K$ are the projection points of $G_2$ in the axial section and X-axis, respectively. Assume $\beta$ is the central angle corresponding to the arc of $G_2N$, $r_\mathrm{c}$ is the radius of the spiral, and $\theta$ is the angle at which the spiral rotates from $G_2$ to $G_1$. In the coordinate system XYZ, the three-dimensional coordinates of $G_2$ can be expressed as (1):

$$\begin{cases} x_{G_2} = d_2/2 + r_\mathrm{b} - r_\mathrm{b}\cos\beta \\ y_{G_2} = -r_\mathrm{b}\sin\beta\sin\varphi \\ z_{G_2} = r_\mathrm{b}\sin\beta\cos\varphi \end{cases} \quad (1)$$

Assuming that $\Delta z_1$ is the difference between $G_1$ and $G_2$ in the direction of the axis, the three-dimensional coordinates of $G_1$ can be expressed as (2):

$$\begin{cases} x_{G_1} = \sqrt{(d_2/2 + r_\mathrm{b} - r_\mathrm{b}\cos\beta)^2 + (\mathrm{r}_b \sin\beta \sin\varphi)^2} \\ y_{G_1} = 0 \\ z_{G_1} = z_{G_2} + \Delta z_1 \end{cases} \quad (2)$$

Assuming that $p$ is the lead of the ball screw, then in the coordinate system UVW, points $G_1$ and $G_2$ can be expressed as (3) and (4):

$$\begin{cases} u_{G_1} = r_\mathrm{c}\cos\theta_{G_1} \\ v_{G_1} = r_\mathrm{c}\sin\theta_{G_1} \\ w_{G_1} = \frac{p\cdot\theta_{G_1}}{2\pi} \end{cases} \quad (3)$$

$$\begin{cases} u_{G_2} = r_\mathrm{c}\cos\theta_{G_2} \\ v_{G_2} = r_\mathrm{c}\sin\theta_{G_2} \\ w_{G_2} = \frac{p\cdot\theta_{G_2}}{2\pi} \end{cases} \quad (4)$$

The correspondence between $G_1$ and $G_2$ in coordinate systems XYZ and UVW is shown in (5):

$$\begin{cases} x_{G_1} = u_{G_1} \\ x_{G_2} = u_{G_2} \\ \Delta z_1 = w_{G_1} - w_{G_2} \end{cases} \quad (5)$$

According to equations (1)-(5), the thread profile of the ball screw in the axial section in the coordinate system XYZ is as (6):

$$\begin{cases} x = \sqrt{(d_2/2 + r_\mathrm{b} - r_\mathrm{b}\cos\beta)^2 + (r_\mathrm{b}\sin\beta\sin\varphi)^2} \\ y = 0 \\ z = r_\mathrm{b}\sin\beta\cos\varphi + \frac{p}{2\pi}\arccos((d_2/2 + r_\mathrm{b} - r_\mathrm{b}\cos\beta)/x) \end{cases} \quad (6)$$

In addition, the differential equation between the theoretical thread profile in the axial section and the theoretical thread profile in the normal section along the Z-axis is as (7).

So far, the equation of the theoretical thread profile in the axial section is obtained, and the transformation relationship between it and the theoretical thread profile in the normal section is obtained.

$$\begin{cases} \Delta z_1 = \frac{p}{2\pi}\arccos((d_2/2 + r_\mathrm{b} - r_\mathrm{b}\cos\beta)/r_\mathrm{c}) \\ \cos\beta = \frac{-r_\mathrm{b}d_2 + \sqrt{{r_\mathrm{b}}^2{d_2}^2 - 4{r_\mathrm{b}}^2(1+(\sin\varphi)^2)\left(x^2 - \left(\frac{d_2}{2}\right)^2 - r_\mathrm{b}d_2 - {r_\mathrm{b}}^2(1+(\sin\varphi)^2)\right)}}{2{r_\mathrm{b}}^2(1+(\sin\varphi)^2)} \end{cases} \quad (7)$$

## 4. THEORETICAL THREAD PROFILE PROJECTION CURVE IN AXIAL SECTION AND CORRECTION ALGORITHM

As mentioned in Section 2, the outline captured by the CCD camera is not the actual thread profile in the axial section of the ball screw because it is blocked by the shadow area generated by the helix spiraling upward. Therefore, in this section, the reasons for the occlusion of the thread profile in the axial section are analyzed and the equation of the theoretical profile projection curve in the axial section is obtained and solved.

### *4.1 Equation of thread profile projection curve in axial section*

In order to find out the reason why the points on the ball screw profile curve are blocked by other points, three spiral lines of the thread profile raceway $l_3$、$l_4$ and $l_5$ are specifically taken, as shown in Fig. 9.

Where $B_0$ is the intersection point between the upper edge of the thread raceway and the axial section, $M_0$ and $C_0$ are two points of the axis section curve, and $Z_{B_0} > Z_{C_0} > Z_{M_0}$. $B$, $C$ and $M$ are respectively obtained from $B_0$, $C_0$, $M_0$ spirally rising angles of $\theta_B$, $\theta_C$ and π. Assume $M$ is a point on the profile in the axial section, and the coordinate values of $B$, $C$ and $M$ on the Z-axis are equal to $X_M$. Therefore, the coordinate values of $B$, $C$ and $M$ on the Z-axis can be expressed as (8):

$$\begin{cases} Z_B = Z_{B_0} + \frac{P}{2\pi}\left(\pi - \arccos\frac{2X_M}{d_1}\right) \\ Z_C = Z_{C_0} + \frac{P}{2\pi}\left(\pi - \arccos\frac{X_M}{X_C}\right) \\ Z_M = Z_{M_0} + \frac{P}{2} \end{cases} \quad (8)$$

From (8), $Z_B$ is an increasing function of $X_M$, and the monotonicity of $Z_C$ first decreases and then increases. So the magnitude relationship between $Z_B$、$Z_C$ and $Z_M$ is uncertain. The results show that $M$ will be blocked by $C$ when $Z_C = \min\{Z_M, \min Z_C, Z_B\}$, and the point of the projection boundary corresponding to $M$ is $C$. Also, $M$ will be blocked by $B$ when $Z_B = \min\{Z_M, \min Z_C, Z_B\}$, and the point of the projection boundary corresponding to $M$ is $B$.

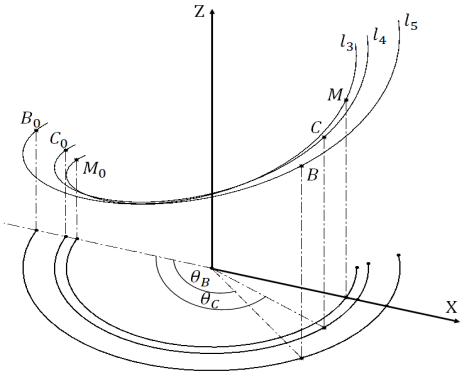


Fig. 9. Occlusion analysis of the thread profile in the axial section.

The differential equation $\Delta z_2$ between the thread profile and the projection curve in the axial section can be obtained from equations (6)-(9), as shown in (10).

$$z_2 = \begin{cases} \min Z_\mathrm{C} & if\ \min Z_C \le Z_B \\ Z_B & if\ \min Z_C > Z_B \end{cases} \quad (9)$$

$$\Delta z_2 = z_2 - z \quad (10)$$

### *4.2 Solving thread profile projection curve based on Linear Search*

According to (9) and (10), $Z_C$ must be optimized and it is assumed that $y = Z_C$. From (10) it is evident that the search for the optimal value of $y$ is a typical One-Dimensional Optimization problem, as in [19], which can be solved by the Linear Search [20]. The Linear Search method can be divided into two stages: First, the search interval containing the optimal solution of the problem is determined. Second, segmentation or interpolation is used to narrow the interval. The Golden-Section algorithm is adopted here, as in [21]-[23], the golden ratio $\lambda = \frac{\sqrt{5}-1}{2}$ and the precision $\delta = 10^{-10}$. First set the initial state value: $a$, $b$, $x_1$ and $x_2$, then compute $\beta_1, \beta_2, y_1, y_2$ and $\delta_2$. Next, update the state or obtain $y^*$. The solution process is shown in Fig. 10.

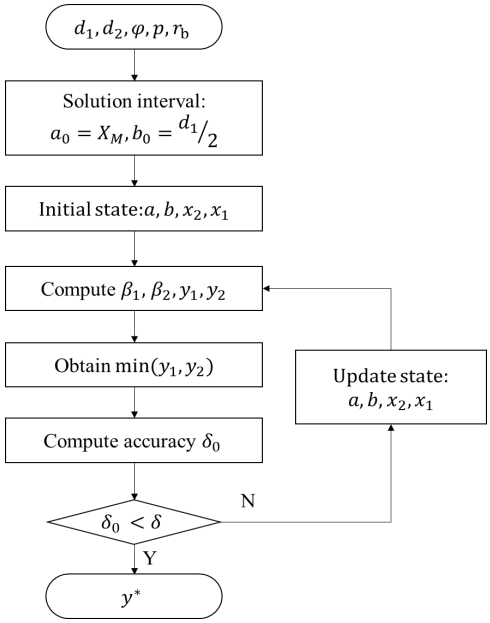


Fig. 10. Solving process based on the Linear Search.

### *4.3 Correction algorithm of thread profile projection curve*

Table 1 shows the steps of the correction algorithm. Through Step 1 to Step 4, the differential equation between the thread profile and the thread profile projection curve in the axial section can be obtained, which is the theoretical basis for Step 5.

Table 1. Correction steps of thread profile projection curve.

| | |
|---|---|
| **Step1:** | Substitute the ball screw parameters, and solve the equation of $\boldsymbol{Z_B}$ in (9). |
| **Step2:** | Take multiple discrete points along the X-axis, and for each point, solve the optimal value of $Z_C$ in (9). |
| **Step3:** | Perform curve fitting on the points obtained in Step 2 to obtain the equation of $\min Z_C$ in (9). |
| **Step4:** | Find the intersection of the two equations of Step1 and Step3 to obtain the difference equation that is segmented by the intersection point. |
| **Step5:** | Conduct the correction of thread profile projection curve based on the differential equation in Step4, and get the actual thread profile in the axial section. |

## 5. CORRECTION OF ACTUAL THREAD PROFILE PROJECTION CURVE AND EXPERIMENTS

Capturing the thread profile projection curve of the axial section with a CCD camera and reconstructing it with the correction method in section 4.3, the actual thread profile in the axial section can be obtained. Based on this, key parameters of the ball screw thread can be measured. By comparing them with theoretical values, the detection result on the thread quality can be assessed.

### *5.1 Visual detection system for ball screw thread profile*

A visual detection system for a ball screw thread is designed for experiment, the overall structure of this system is shown in Fig. 11.

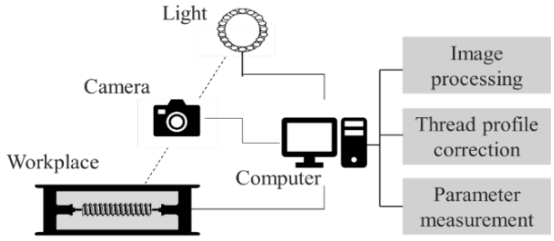


Fig. 11. Structure of the visual detection system.

The hardware of the detection system includes workstation, light and camera: the workstation is used to automatically clamp the ball screw; the light is used to provide suitable illumination to the ball screw to ensure the quality of the captured images; and the camera or CCD can convert the obtained image signal into a digital signal, providing a basis for the next image processing and thread profile correction.

The software of the detection system also includes three main modules: image preprocessing, thread profile projection curve correction, and parameter measurement. The image preprocessing module includes image filtering, binarization and contour extraction; the thread profile projection curve correction module integrates the algorithm proposed above to correct the actual projection curve; the parameter measurement module measures the key parameters of the thread profile and supports the detection result.

### *5.2 Correction of actual thread profile projection curve in axial section*

The ball screw of model FN5010-6 was selected as the experimental object, and its profile parameters are shown in Table 2.

Table 2. Parameter table of FN5010-6.

| Parameter /unit | Outer diameter /mm | Pitch /mm | Lead angle /° | Adapted ball diameter /mm |
|---|---|---|---|---|
| Value | 49 | 10 | 3.8965 | 5.953 |

First, the image of the ball screw obtained by a CCD camera was preprocessed to extract the thread profile projection curve in the axial section, the result is shown in Fig. 12.

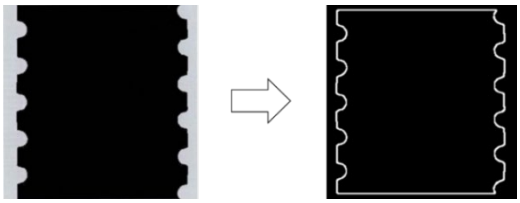

Fig. 12. Comparison before and after image processing.

Then, selecting a segment of the thread profile projection curve to modify according to the method described in Section 4.3, the differential equation between the theoretical thread profile and the theoretical thread profile projection curve in the axial section was obtained as Curve-3 in Fig. 13. The actual thread profile projection curve is Curve-4, and the corrected actual thread profile in the axial section is Curve-5. There is a significant difference between the thread profile and the thread profile projection curve.

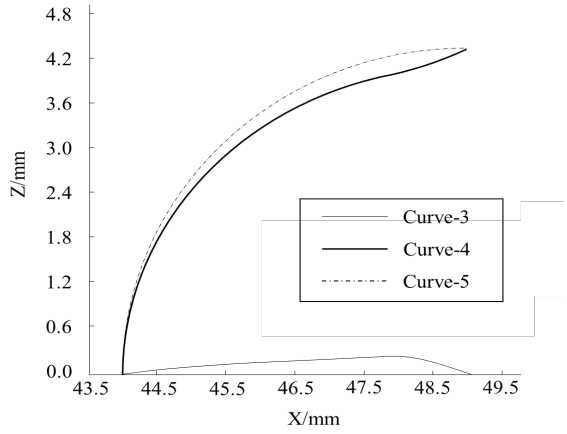


Fig. 13. Comparison before and after curve correction.

### *5.3 Acquisition of actual thread profile in normal section*

Take discrete points on the curve of the actual profile in the axial section obtained above in chapter 5.2, adopt (7) to find the difference between the thread profile in the axial section and the theoretical thread profile in the normal section at each point on the Z-axis.

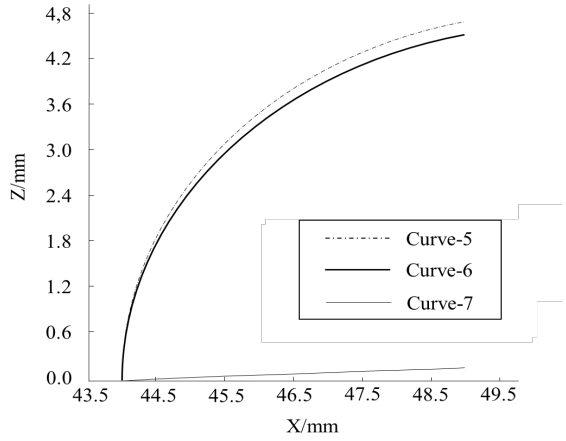


Fig. 14. Comparison between the actual thread profile in the axial section and in the normal section.

Then perform curve fitting. The differential equation curve obtained is Curve-7 in Fig. 14, and the actual thread profile in the normal section is derived as shown in Curve-6. Then the fitting circle radius of the theoretical thread profile in the normal section can be calculated.

### *5.4 Results and analysis*

There are two main aspects to test if the thread profile of a ball screw is qualified. On the one hand, the standard parameters such as outer diameter and pitch are measured and compared. On the other hand, the radius of the normal fitting circle and that of the thread profile are compared and it can be assessed whether the error is within the allowable tolerance range.

The experiment combines the above two aspects for detection and analysis. The parameters were measured with the uncorrected thread profile curve, which is exactly the thread profile projection curve in the axial section (Curve-4), and the corrected thread profile curve in the axial section (Curve-5). The results are shown in Table 3.

Table 3. Comparison of the thread profile between Theoretical results and Measured results.

| Para-meters | Theoretical values | Curve-4 | | Curve-5 | |
|---|---|---|---|---|---|
| | | Measured values | Error | Measured values | Error |
| $d_1$ [mm] | 49.0000 | 49.0343 | 0.0343 | 49.0302 | 0.0302 |
| $p$ [mm] | 10.0000 | 9.9765 | -0.0235 | 9.9815 | -0.0185 |
| $\varphi$ [°] | 3.8965 | 3.8036 | -0.0929 | 3.8858 | -0.0107 |
| $r_b$ [mm] | 3.0956 | 3.0224 | 0.0732 | 3.0876 | 0.0080 |

Table 2 shows that: (1) Compared with the thread profile projection curve in the axial section and the intersection line in the normal section before correction, the measurement errors of the thread profile curve in the axial section after correction are all smaller, especially the lead angle and the fitting radius of the normal circle are reduced by more than 80%. (2) Whether the thread profile curve is corrected has little effect on the measured values of the outer diameter and pitch.

It can be concluded from these two results that correcting the thread profile projection curve in the axial section captured by the camera without adjusting the shooting angle can significantly improve the accuracy of profile detection, which verifies the effectiveness and superiority of the thread profile detection method.

## 6. CONCLUSIONS

When machine vision is used for ball screw thread profile detection, an error in the angle adjustment occurs when the camera is tilted to shoot the normal section. When the camera shoots the thread profile of the axial section orthogonally, the actual thread profile in the axial section cannot be directly obtained due to the phenomenon of occlusion of the tooth profile projection. The main work of this paper is as follows:

1. A ball screw thread profile detection method based on the thread profile in the axial section is proposed, which avoids the angle adjustment error that may be caused when the camera captures the normal section.
2. The theoretical models of the thread profile in the normal section, the thread profile in the axial section and the thread profile projection curve in the axial section of the ball screw are established, and the solution and correction methods of the thread profile projection curve in the axial section are proposed.
3. In the experiment, a CCD camera was used to obtain the actual thread profile projection curve in the axial section, and the solution and correction were performed to obtain the actual thread profile in the axial section and the actual thread profile in the normal section. Based on this, the key parameters of the profile were measured and the error analysis was performed. The lead angle and the fitting radius of the thread profile in the normal section were reduced by more than 80%.

The results show that the thread profile detection method proposed in this paper can improve the accuracy of thread profile detection and has high theoretical value.

## REFERENCES


[1] Cheng, Q., Qi, B., Liu, Z., Zhang, C., Deyi, X. (2019). An accuracy degradation analysis of ball screw mechanism considering time-varying motion and loading working conditions. *Mechanism and Machine Theory*, 134, 1-23. https://doi.org/10.1016/j.mechmachtheory.2018.12.024

[2] Altintas, Y., Yang, J., Kilic, Z. M. (2019). Virtual prediction and constraint of contour errors induced by cutting force disturbances on multi-axis CNC machine tools. *CIRP Annals*, 68 (1), 377-380. https://doi.org/10.1016/j.cirp.2019.04.019

[3] Gadelmawla, E. S. (2017). Computer vision algorithms for measurement and inspection of external screw threads. *Measurement*, 100, 36-49. https://doi.org/10.1016/j.measurement.2016.12.034

[4] Wang, Y., Zhang, C., He, Y., Tao, L., Feng, H. (2018). Development and evaluation of non-contact automatic tool setting method for grinding internal screw threads. *The International Journal of Advanced Manufacturing Technology*, 98 (1), 741-754. https://doi.org/10.1007/s00170-018-2258-5

[5] Perng, D., Chen, S., Chang, Y. (2010). A novel internal thread defect auto-inspection system. The International Journal of Advanced Manufacturing Technology, 47 (5), 731-743. https://doi.org/10.1007/s00170-009-2211-8

[6] Martínez, S. S., Vázquez, C. O., García, J. G., Ortega, J. G. (2017). Quality inspection of machined metal parts using an image fusion technique. *Measurement*, 111, 374-383. https://doi.org/10.1016/j.measurement.2017.08.002

[7] Jing, M., Du, Y. (2020). Flank angle measurement based on improved Sobel operator. *Manufacturing Letters*, 25, 44-49. https://doi.org/10.1016/j.mfglet.2020.07.002

[8] Zhen, N., An, Q. (2018). Analysis of stress and fatigue life of ball screw with considering the dimension errors of balls. *International Journal of Mechanical Sciences*, 137, 68-76. https://doi.org/10.1016/j.ijmecsci.2017.12.038

[9] Min, J. (2018). Measurement method of screw thread geometric error based on machine vision. *Measurement & Control*, 51 (7-8), 304-310. https://doi.org/10.1177/002029401878675

[10] Zhao, L., Feng, H., Rong, Q. (2018). A novel non-contact measuring system for the thread profile of a ball screw. *Mechanical* Sciences, 9 (1), 15-24. https://doi.org/10.5194/ms-9-15-2018

[11] Wang, K., Feng, H. T. (2020). Optimization measurement for the ballscrew raceway profile based on optical measuring system. *Measurement Science and Technology*, 32 (3), 035010. https://doi.org/10.1088/1361-6501/abc3de

[12] Senthilnathan, R., Nandhini, M., Ranjani, R., Sridevi, S. (2017). Vision based orientation invariant measurement of metric screw thread parameters. In *2017 Trends in Industrial Measurement and Automation (TIMA)*. IEEE, 1-5. https://doi.org/10.1109/TIMA.2017.8064811

[13] Liu, C. Y., Yen, T. P. (2016). Digital multi-step phase-shifting profilometry for three-dimensional ball screw surface imaging. *Optics & Laser Technology*, 79, 115-123. https://doi.org/10.1016/j.optlastec.2015.12.001

[14] Li, Z., Zhang, K., Wu, J., Lu, P. (2020). External thread measurement based on ResUnet and HMM. In *2020 5th International Conference on Computer and Communication Systems (ICCCS)*. IEEE, 400-403. https://doi.org/10.1109/ICCCS49078.2020.9118595

[15] Chen, M. L. (2018). Compensation of thread profile distortion in image measuring screw thread. *Measurement*, 129, 582-588. https://doi.org/10.1016/j.measurement.2018.07.041

[16] Liu, C., He, Y., Li, Y., Wang, Y., Wang, L., Wang, S., Wang, Y. (2021). Predicting residual properties of ball screw raceway in whirling milling based on machine learning. *Measurement*, 173, 108605. https://doi.org/10.1016/j.measurement.2020.108605

[17] Chen, J. H., Zhang, J. J., Gao, R. J., Jiang, C.H., Ma, R., Qi, Z.M., Jin, H., Zhang, H.D., Wang, X.C. (2020). Research on modified algorithms of cylindrical external thread profile based on machine vision. *Measurement Science Review*, 20 (1),15-21. https://doi.org/10.2478/msr-2020-0003

[18] Cavoretto, R., De Rossi, A., Mukhametzhanov, M. S., Sergeyev, Y.D. (2021). On the search of the shape parameter in radial basis functions using univariate global optimization methods. *Journal of Global Optimization*, 79 (2), 305-327. https://doi.org/10.1007/s10898-019-00853-3

[19] Czyzowicz, J., Georgiou, K., Kranakis, E. (2019). Group search and evacuation. In *Distributed Computing by Mobile Entities*. Springer, 335-370. https://doi.org/10.1007/978-3-030-11072-7_14

[20] Mukhametzhanov, M. S., Cavoretto, R., De Rossi, A. (2020). An experimental study of univariate global optimization algorithms for finding the shape parameter in radial basis functions. In *Optimization and Applications: 10th International Conference OPTIMA 2019*. Springer, 1145, 326-339. https://doi.org/10.1007/978-3-030-38603-0_24

[21] Li, K., Wang, Q., Wang, M., Han, Y. (2019). Imaging of a distinctive large bubble in gas–water flow based on a size projection algorithm. *Measurement Science and Technology*, 30 (9), 094004. https://doi.org/10.1088/1361-6501/ab16b0

[22] Huang, P., Liu, C., Yang, X., Yi, D., Zhang, H. (2022). High-speed measurement system for cord-rubber composites on conveyor belt based on machine vision. In *5th International Conference on Informatics Engineering and Information Science (ICIEIS 2022)*. SPIE, 1245209, 62-68. https://doi.org/10.1117/12.2662333

[23] Wang, C. S., Kao, I. H., Hsu, Y. W., Lin, T. C., Tsay, D. M. (2021). Thread quality classification of a tapping machine based on machine learning. *IEEE Transactions on Instrumentation and Measurement*, 70, 1-15. https://doi.org/10.1109/TIM.2021.3067216

Received August 19, 2022
Accepted January 22, 2023